The Bipolar Field-Effect Transistor: V. Bipolar Electrochemical Current Theory (Two-MOS-Gates on Thin-Base)*

Jie Binbin[1,†] and Sah Chih-Tang[1,2,3,†]

(1 *Peking University*, *Beijing* 100871, *China*)
(2 *University of Florida*, *Gainesville*, *Florida* 32605, *USA*)
(3 *Chinese Academy of Sciences*, *Foreign Member*, *Beijing* 100864, *China*)

Abstract: This paper reports the intrinsic-structure DC characteristics computed from the analytical electrochemical current theory of the bipolar field-effect transistor (BiFET) with two identical MOS gates on nanometer-thick pure-base of silicon with no generation-recombination-trapping. Numerical solutions are rapidly obtained for the three potential variables, electrostatic and electron and hole electrochemical potentials, to give the electron and hole surface and volume channel currents, using our cross-link two-route or zig-zag one-route recursive iteration algorithms. Boundary conditions on the three potentials dominantly affect the intrinsic-structure DC characteristics, illustrated by examples covering 20-decades of current (10^{-22} to 10^{-2} A/Square at $400cm^2/(V \cdot s)$ mobility for 1.5nm gate-oxide, and 30nm-thick pure-base). Aside from the domination of carrier space-charge-limited drift current in the strong surface channels, observed in the theory is also the classical drift current saturation due to physical pinch-off of an impure-base volume channel depicted by the 1952 Shockley junction-gate field-effect transistor theory, and its extension to complete cut-off of the pure-base volume channel, due to vanishing carrier screening by the few electron and hole carriers in the pure-base, with Debye length (25mm) much larger than device dimension (25nm).

Key words: bipolar field-effect transistor theory; recursive iteration; electron and hole electrochemical potentials; electric potential; boundary conditions
PACC: 7340Q **EEACC**: 2560S; 2560B
CLC number: TN386.1 **Document code**: A **Article ID**: 0253-4177(2008)04-0620-08

1 Introduction

In three previous reports, 0, I and III[1~3], we presented the one-section and two-section electrochemical potential theory of the DC current-voltage (DCIV) and conductance-voltage (DCgV) characteristics of the recently discovered bipolar currents (simultaneous presence of electron and hole surface and volume channel currents) in nanometer field effect transistors with two identical MOS gates on thin pure silicon base known as FinFETs[1]. We renamed the 55-year-old unipolar field effect transistor (UniFET), coined by Shockley in 1952[4], the bipolar field effect transistor (BiFET), on account of this new, bipolar, mode of operation. We noticed and stated that the bipolar mode is a simultaneous presence of both electron and hole channels in any combinations of single or multiple surface and volume channels. We also noted that the bipolar mode is universally present in all types, compositions and structures, of field effect transistors by virtual that semiconductor is a two-carrier-species (electron and hole) conductor of electricity, that is controlled by one or more transverse electric fields of the field-effect gates.

Numerical recursive iteration solutions, terminated at the initial guess of the unipolar solution, were given in these three reports[1~3] to illustrate the effects of base silicon and gate oxide thicknesses on the bipolar DCIV characteristics, from which it was stipulated on simple device physics that the bipolar DCIV and DCgV could deviate significantly from the unipolar solutions, only when the two unipolar (electron or hole) currents are comparable. This report presents a continuation of our study to understand the electrical properties of the FinFET in view of its eminent position and promise as the future MOS transistor[5], especially to illustrate the importance of the boundary and internal conditions on the DC characteristics of the intrinsic transistor since the boundary conditions are in fact simulations of the real transistors containing the two contacts to the two ends of the base-body channel[6]. The rigorously derived gov-

* This investigation and Jie Binbin have been supported by the CTSAH Associates (CTSA), founded by the late Linda Su-Nan Chang Sah, in memory of her 70th year.
† Corresponding author. Email: bb_jie@msn.com and tom_sah@msn.com
Received 25 March 2008, revised manuscript received 28 March 2008
©2008 Chinese Institute of Electronics

erning DC steady-state equations given in the report last month[7], used in the preceding paper[6], are again used as the starting equations in this report.

2 Electrochemical Potential Theory

The DC electrical characteristics are governed by three DC steady-state equations (Poisson and Electron and Hole Continuity Equations) given by (1) to (3) below in pure-silicon ($P_{IM}=0$) with no electron-hole generation-recombination-trapping ($G_N=R_N=G_P=R_P=0$)[6,7]

$\nabla\cdot(\varepsilon_S \boldsymbol{E})=\rho(x,y,z)=q(P-N-P_{IM})=q(P-N)$ 3-D Poisson Equation (1)

$\nabla\cdot\boldsymbol{J}_N=-q(G_N-R_N)=0$ 3-D Electron Current Continuity Equation (2)

$\nabla\cdot\boldsymbol{J}_P=+q(G_P-R_P)=0$ 3-D Hole Current Continuity Equation (3)

$[-(\partial^2 U/\partial X^2)-(L_D/L)^2(\partial^2 U/\partial Y^2)]=[\exp(U_P-U)-\exp(U-U_N)]/2$ 2-Dimensional (4)

$\int J_{NX}\partial yZ+\int J_{NY}\partial xZ=\textbf{constant}=-I_N$ 2-Dimensional (5)

$\int J_{PX}\partial yZ+\int J_{PY}xZ=\textbf{constant}=-I_P$ 2-Dimensional (6)

In (4)～(6), the Cartesian Coordinates is employed which is defined by $\boldsymbol{r}=\boldsymbol{i}_x x+\boldsymbol{i}_y y+\boldsymbol{i}_z z$ with the differential volume element $d\mho=dxdydz$. The transistor is scaled by normalizing the base thickness and x-variable to the pure-silicon-base Debye Length, $X=x/L_D$ where $L_D=(\varepsilon_{Si}k_BT/2qn_i)^{1/2}$, the base or channel length and the y-variable to the Channel Length, $Y=y/L$, and the z-variable to the Channel width, $Z=z/W$ and the properties are assumed to be constant in the z-direction. The currents are given as the sheet current in Ampere per Square, where 1 Square is $W/L=1$. The carrier concentrations are represented by their electrochemical potentials, $N=n_i\exp(U-U_N)$ and $P=n_i\exp(U_P-U)$ where n_i is the intrinsic carrier concentration, $\sim 1.333484\times10^{10}$ cm^{-3} at $T=300.00$K, $qV_P(x,y,z)/k_BT\triangleq U_P(x,y,z)\equiv U_P(y)$ and $qV_N(x,y,z)/k_BT\triangleq U_N(x,y,z)\equiv U_N(y)$ are the electrochemical potentials of electrons and holes, assumed to be independent of x and z. The solution for the FinFET given below is copied from [7], using the same equation numbers as [7] for convenience. The impurity terms, P_{IM}, and the 2-D terms, $\partial E_Y/\partial Y\sim\partial^2U/\partial Y^2\sim(L_D/L)^2$, are deleted in the present paper which are studied in a future report.

Symmetrical-Gate Thin Pure-Base (FinFET)

$$(\partial U/\partial X)^2=F^2(U,U_P,U_N,U_0,P_{IM},E_Y)=+\exp(U-U_N)-\exp(U_0-U_N)+\exp(U_P-U)-\exp(U_P-U_0)-(P_{IM}/n_i)\times(U-U_0)+2(L_D/L)^2\int(\partial^2U/\partial Y^2)\partial_X U \quad (57)$$

$$U_{GS}-U_S=\mathrm{sign}(U_S-U_0)\times(C_D/C_O)\times(\partial U/\partial X)_S \quad \text{(1-D term)}\ (58)$$

$$-(x_O/L)^2\iint_{oxide}(\partial^2U/\partial Y^2)\partial X\partial X-(1/2)(x_O/L_D)^2\iint(\rho_{oxide}/qn_i)\partial X\partial X \quad \text{(2-D terms)}\ (59)$$

$$X_B=2\int\mathrm{sign}(U-U_0)\partial_X U/F \quad \text{(Integrated from } U=U_S \text{ to } U=U_0\text{) (The Thickness Equation) (60)}$$

The general current and Y equations are

$$I_N=+qD_n n_i(W/L)L_D(\partial U_N/\partial Y)\exp(-U_N)\int\exp(+U)\partial_X U/F(U,U_P,U_N,U_0,P_{IM},E_Y) \quad (61)$$

$$=+qD_n n_i(W/L)L_D\int\partial_Y U_N\exp(-U_N)\int\exp(+U)\partial_X U/F(U,U_P,U_N,U_0,P_{IM},E_Y) \quad (62)$$

$$I_P=+qD_p n_i(W/L)L_D(\partial U_P/\partial Y)\exp(+U_P)\int\exp(-U)\partial_X U/F(U,U_P,U_N,U_0,P_{IM},E_Y) \quad (63)$$

$$=+qD_p n_i(W/L)L_D\int\partial_Y U_P\exp(+U_P)\int\exp(-U)\partial_X U/F(U,U_P,U_N,U_0,P_{IM},E_Y) \quad (64)$$

The y-variation equations to give $U_N(y)$, $U_P(y)$, $U_S(y)$ and $U_0(y)$, and their derivatives, $\partial/\partial y$, are obtained by integration in Y using the y-independence of I_N and I_P.

$$I_N=+qD_n n_i(W/L)[L_D/(Y)]\int\partial_Y U_N\exp(-U_N)\int\exp(+U)\partial_X U/F(U,U_P,U_N,U_0,P_{IM},E_Y) \quad (65)$$

$$I_P=+qD_p n_i(W/L)[L_D/(1-Y)]\int\partial_Y U_P\exp(+U_P)\int\exp(-U)\partial_X U/F(U,U_P,U_N,U_0,P_{IM},E_Y) \quad (66)$$

The location of the flatband plane, $y=y_0$, that divides the two sections is given by any one of

$$(y_0/x_B)=(\partial U_{N0}/\partial y)\cdot\exp(U_0-U_{N0})/\int(\partial U_N/\partial y)\partial y\int\exp(U-U_N)\partial x \ (x=0 \text{ to } x_B;\ y=0 \text{ to } y_0) \quad (67)$$

$$(L-y_0)/x_B=(\partial U_{N0}/\partial y)\cdot\exp(U_0-U_{N0})/\int(\partial U_N/\partial y)\partial y\int\exp(U-U_N)\partial x \ (x=0 \text{ to } x_B;\ y=y_0 \text{ to } L) \quad (68)$$

$$(L-y_0)/x_B = (\partial U_{P0}/\partial y)\cdot \exp(U_{P0}-U_0)/\int(\partial U_P/\partial y)\partial y\int \exp(U_P - U)\partial x \quad (x=0 \text{ to } x_B; y=y_0 \text{ to } L) \quad (69)$$

$$(y_0/x_B) = (\partial U_{P0}/\partial y)\cdot \exp(U_{P0} - U_0)/\int(\partial U_P/\partial y)\partial y\int \exp(U_P - U)\partial x \quad (x = 0 \text{ to } x_B; y = 0 \text{ to } y_0) \quad (70)$$

3 Computed Current-Voltage Characteristics

3.1 Recursive Iteration Algorithms

We need to have three internal relationships ($0<Y<1$) between the four potential variables, $U_S(Y)$, $U_0(Y)$, $U_N(Y)$ and $U_P(Y)$ in order to obtain the electron and hole currents, I_N and I_P, from either the single integration of $\int dx$ or $\int \partial_X U$ combined with the gradient $\partial_Y U_N/\partial Y$ and $\partial_Y U_P/\partial Y$ given respectively by (61) and (63), or the double integrations of $\iint dxdy$ or $\iint \partial_X U \partial_Y U_N$ and $\iint \partial_X U \partial_Y U_P$, (62) and (64). $U_0(Y)$ may be used as the integration variable, then $\partial_Y U_N/\partial_Y U_0$ and $\partial_Y U_P/\partial_Y U_0$ need to be evaluated analytically or numerically. Use of $U_0(Y)$ may be advantageous because it has the fundamentally justified and simply defined boundary conditions, which actually corresponds to the intrinsic-structure transistor with unrestricted contacts at the two ends of the channel: $U_0(Y=0) = U_{SB} \triangleq qV_{SB}/k_BT = 0$ at the source contact point $S(x=x_B/2, y=0, z=0 \text{ to } W)$, and $U_0(Y=1) = U_{DB} \triangleq qV_{DB}/k_BT$ at the drain contact point $D(x=x_B/2, y=L, z=0 \text{ to } W)$. Here V_{DB} and V_{SB} are the DC voltages applied to the drain contact point $D(x_B/2, L, z)$ and source contact point $S(x_B/2, 0, z)$ relative to the electric potential reference point $B(x, y, z)$. However, there are only two explicit internal relationships: (i) the voltage equation given by (58)-(59) using (57) for the transverse electric field, $F \propto E_X$, and (ii) the base-thickness equation given by (60) using (57) for the transverse electric field F. The third relationship is generated during the recursive iteration, which relates N and P to the divergence of the electric field, or the electrical displacement, $\nabla\cdot\boldsymbol{D}\equiv\nabla\cdot(\varepsilon\boldsymbol{E})$, or which relates U_N, U_P and U, given by (1), the Poisson Equation.

Thus, the recursive iterations, indicated by the subscript number index r, may be started using the unipolar approximation ($r=0$) of the voltage equation, (58)-(59), and thickness equation (60), both using (57) for the x-component of the electric field, $\partial_X U/\partial X$. As an example, consider the n-channel or the positive voltages applied to all four terminals (actually boundaries), S, D, G1 = G2 = G, or $U_{DS}\gtreqless U_{GS}\geqslant 0$. Then from these two internal-condition equations, the relationships of $U_S(U_N)$ and $U_0(U_N)$ can be obtained numerically by successive approximation or iteration, to be denoted by the subscript i (not the recursive iteration number r), or analytically since there are no holes for this initial-guess solution, i.e. the unipolar solution. Then, the unipolar electron current density, I_{Nr} ($r=0$ for the initial unipolar solution), can be obtained by numerical evaluation of the single integral (61) or double integral (62). The convergent solution from the i-th iteration or the analytical solution also gives $U_{Nr}(Y)$, $U_{Sr}(Y)$ and $U_{0r}(Y)$, with $r=0$. This successive iteration is also carried out for the unipolar hole current density, I_{Pr} (with $r=0$) and the three potentials $U_{Pr}(Y)$, $U_{Sr}(Y)$ and $U_{0r}(Y)$, with $r=0$. If the successive iterations are carried to completion, the two sets of electric potentials $U_{Sr}(Y)$ and $U_{0r}(Y)$, one from computing the electron current and one from computing the hole current, should be equal numerically for $r=0$, but also for any higher recursive iteration cycle, $r>0$. So, let us denote the recursive iterations by the labels Nr and Pr where N stands for electron current as the majority and P stands for hole current as the majority, and r is the number of recursive iteration or the recursive iteration cycle number. The complete set contains six members: two currents which are the end results and four potentials, three of which are iterated to find their values or to find the values of the two potentials in terms of the third potential using the two internal condition equations, the voltage equation (58)-(59)-(57) and the thickness equation (60)-(57), so that the two currents can computed as the end results of the specific recursive iteration cycle, r. The six members of the set, $(I_{Nr}, I_{Pr}, U_{Nr}, U_{Pr}, U_{Sr}, U_{0r})$, are split into four majority carrier terms and two minority carrier terms. The minority carrier electrochemical potential is fixed during the iteration and its value at each Y comes from the previous recursive iteration. For example, in the $Nr+1$-th recursive iteration cycle, the minority carrier hole electrochemical potential at each Y_j, $U_{Pr}(Y_j)$ for $0\leqslant Y_j\leqslant 1$ is fixed to the value obtained from the previous recursive iteration cycle, U_{Pr}. Here j could be 100 or 1000 equal or unequal ΔY_j's with which the channel is divided into to facilitate the numerical integration and differentiation. In order to delineate the fixed value, a third numerical subscript f is added. For example, in the Nr-th recursive iteration, for the electron majority carrier, we

have the four electron majority carrier terms of I_{Nr}, U_{Nr}, U_{Sr}, and U_{0r}, and the two hole minority carrier terms, U_{Prf} and I_{Prf}. $r=0$ denotes initial guess which in this case, is the unipolar electron solution with $P=0$. Thus, initial guess in the initial cycle of this recursive iteration algorithm, $r=0$, gives the unipolar electron solution, converged at the i-th successive iteration, at the applied terminal (actually "boundary") voltages of (V_{GB}, V_{SB}, V_{DB}), to be denoted by I_{N0}, $U_{N0}(Y)$, $U_{S0}(Y)$, $U_{00}(Y)$. The same initial guess procedure gives the unipolar or initial guess for holes, I_{P0}, $U_{P0}(Y)$, $U_{S0}(Y)$, $U_{00}(Y)$. When carried to i-th successive iteration to reach sufficient accuracy in this recursive iteration cycle, the two sets of U_{S0} and U_{00} should be equal. The next recursive iteration cycle, $r=1$, uses the minority carrier solution of the previous iteration, $r=0$, which is fixed and not iterated so denoted by additional subscript f. Thus, the set of $r=1$ solution at a given Y_j is the initial or first order bipolar solution. They are denoted by $N1\{I_{N1}, U_{N1}(Y), U_{S1}(Y), U_{01}(Y), U_{P0f}(Y), I_{P1f}\}$, and $P1\{I_{P1}, U_{P1}(Y), U_{S1}(Y), U_{01}(Y), U_{N0f}(Y), I_{N1f}\}$. The recursive iteration cycle can then be carried on and stopped at the r-th cycle when the user specified convergence criteria are reached, for example, the electron and hole currents change less than 0.001% or some such accuracy. The above description gives a sample recursive iteration algorithm, which is cross-linked between (Nr; Pr) and ($Nr+1$; $Pr+1$), like a symmetrical twisted double-string (double-route) denoted by ($Nr \rightarrow Pr+1 \rightarrow Nr+2 \rightarrow Pr+3 \rightarrow \cdots$; $Pr \rightarrow Nr+1 \rightarrow Pr+2 \rightarrow Nr+3 \cdots$). It is obvious that there are other recursive iteration algorithms, which might be faster but not symmetrical so harder to FORTRAN program, such as the Zig-Zag or ZZ-linked asymmetrical single-route ($Nr \rightarrow Pr \rightarrow Nr+1 \rightarrow Pr+1 \rightarrow Nr+2 \rightarrow Pr+3 \rightarrow \cdots$). It is also obvious that the end results of electron and hole currents at a given recursive iteration cycle should be identical in the symmetrical cross-linked twisted double-string algorithm, while not identical in the asymmetrical zig-zag single-string algorithm, with the last current, say I_{Pr}, always more accurate than the previous current, I_{Nr-1}. This unequal accuracy from unequal recursive iteration cycles in the zig-zag algorithm was indeed observed in our numerical computations.

The device physics basis of the foregoing recursive iteration algorithms is of significant importance. There are three salient features that have been missed by all transistor and device investigators since the Shockley inventions of the 1949 bipolar junction transistors[8] and the 1952 junction-gate field-effect transistor[4].

The first two salient features are related to the electrons and holes. The unrestricted electrochemical potentials of electrons and holes, both internal and at the contact points and contact boundaries, mean that electron and hole currents are not limited by the extrinsic devices, or indeed the computed characteristics are the very characteristics of the intrinsic(-structure) transistor. This has been the case of all transistor and device theories, invented by Shockley, presented by him in both the 1949 bipolar junction transistor theory[8] and the 1952 two p/n-junction-gate volume-channel field-effect transistor[4]. This important fact has not been recognized by all subsequent transistor investigators and manufacturing engineers. The fundamental and application importance of the extrinsic parts of the transistor structures, treated as an intrinsic part of the MOS field-effect transistor, (By intrinsic transistors, we do not mean pure without impurity, but rather the intrinsic physical structure without considering the structures and compositions or types of the contacts to the boundaries.) has only been theoretically and analytically recognized by us twelve months ago (March 2007[1]) when it was noted by us that the Debye screening length of the pure silicon, about 25μm at room temperature, is far larger than the dimension of the nanometer two-MOS-gate pure-base silicon field-effect transistor, although the Debye screening length was emphasized 60 years ago by Shockley and shown by him with examples such as a linearly graded p/n junction[8] to analytically delineate the condition of quasi-neutrality. The inability to screen the electrode charge by the insufficiently-dense or low-concentration mobile electron and hole charges, results in a surface-channel conduction threshold voltage that is scaled by the log of the ratio of the Debye Length to the Gate Oxide thickness, and the electrical channel shortening or the prominence of the two channel length sections also determined by the channel length and the Debye Length.

The second implicit fact of device physics from the unrestricted electrochemical potential of the electrons and holes is that the electron and hole spatial distributions, $N(x,y)=n_i\exp[U(x,y)-U_N(x,y)]$ and $P(x,y)=n_i\exp[U_P(x,y)-U(x,y)]$ are indeed also unrestricted and cannot be set by any arbitrary assumptions, only by the electrical potential, $U(x,y)$ applied to the terminal (boundary) electrodes located at (x,y)'s of the intrinsic transistors. The unrestricted electron and hole currents means that the total electron and hole numbers in the volume of the thin-base of the transistor are also unrestricted. For a counter example, in the traditional nMOST, the hole current is set to zero, then the total hole number can-

not be changed (since generation-recombination-trapping are ignored), which poses a serious restriction, actually impossibility in theory, on unlimited hole accumulation and depletion at the silicon surface under the oxide insulated gate electrode because the total number of holes is fixed when there is no source and sink. This constancy of the hole number would affect drastically the electron current. Thus, previous reports at conferences and in journals where the authors set $U_P(x, y)$ = constant or zero, would give wrong numerical solutions and wrong current-voltage characteristics, in the voltage range where hole concentration is significant and not depleted or exhausted.

The third device physics feature of the present algorithm, also missed by all previous transistor investigators, is the fact that the electrical potential is the only fundamental and physical parameter that can be specified, and only at the transistor's terminals (boundaries), and only specified with respect to a reference potential point in space, (x_r, y_r, z_r), which is based on the experimental Coulomb Law of the $1/r^2$ (inverse distance square) force between two point electrical charges, that is derivable from the gradient of a scalar electrical potential by neglecting the magnetic field.

3.2 Current-Voltage Characteristics and Boundary Condition Effects

The V_{GS} variations of the total electron and hole channel currents, I_N and I_P, are shown in Fig. 1 over a range of V_{DS} with a gate oxide electrical thickness of 1.5nm and a pure-silicon base thickness of 30nm. There are two families of curves. One set comes from specifying the electrical potential boundary condition, $U_0(Y=0) = U_{SB} = 0$ at the source contact boundary and $U_0(Y=1) = U_{DB} = (+0.1\text{V to } +1.0\text{V}) \times (q/kT)$ at the drain contact boundary, to be denoted by BC-$U_0(Y=0,1)$ with the electrochemical potentials unrestricted. The second set comes from specifying the boundary values of the electrochemical potential for electrons or holes, namely, $U_N(Y=0) = U_{SB} = 0$ and $U_N(Y=1) = U_{DB} = (+0.1\text{V to } +1.0\text{V}) \times (q/kT)$ for the electron surface and volume channels, denoted by BC-$U_N(Y=0,1)$, and a similar set from specifying $U_P(Y=1,0)$ for the hole surface and volume channels, denoted by BC-$U_P(Y=1,0)$. Both have the electric potential unrestricted. It is obvious that one can go on and on, with additional potential boundary conditions imposed on the three or even all four potentials, U_N, U_P and U_0, and even U_S at the two boundaries of the base channel, $Y=0$ and $Y=1$, actually also the location X, so that the boundary con-

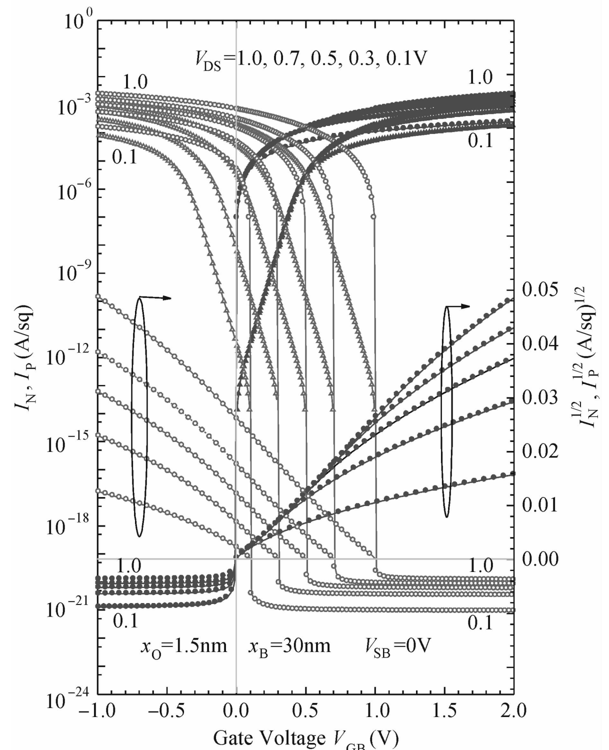

Fig.1 Transfer DC characteristics of a BiFET of two MOS gates and a pure base, with V_{DS} varied. The curves with triangle symbols have the electrochemical potential boundary conditions, while the curves with circle symbols have the electric potential boundary conditions.

ditions are applied to points (X, Y), then, our solution must be extended because it is based on no internal contact points and no boundary contact points except four points at $(X=0, Y=0)$, $(X=0, Y=1)$, $(X = X_B/2, Y=0)$ and $(X = X_B/2, Y=1)$ for the perfectly symmetrical two gates on pure-thin base.

Three salient features each are noted for the surface channel and volume channel currents, all anticipated by "simple" FET device and materials physics, although "anticipation after the facts", after recognizing the device physics of the computer-generated facts. A seventh, verifies the anticipated from recursive iteration algorithm just described.

(1) The currents are higher from the $U_0(Y=0, 1)$ boundary conditions family, BC-U_0, than the currents from the $U_N(Y=0,1)$ and $U_P(Y=0,1)$, families, BC-U_N and BC-U_P. This is understood from the restriction on the electron and hole concentrations and gradients by the BC-U_P and BC-U_N boundary conditions, while the BC-U_0 family of current-voltage curves has no restriction on $U_N(Y)$ and $U_P(Y)$.

(2) The sharp cutoff of the electron and hole currents at flatband of the U_0 boundary conditions, BC-U_0, on the semilog scale, is the result of the well-known parabolic voltage-dependent (shown by $I_N^{1/2}$, $I_P^{1/2}$ on right axis) carrier-space-charge-limited drift

current in surface channel, due to applying the BC only to the electric potential, BC-U_0, obviously also applicable to BC-U_S. The decreasing slope of $I_N^{1/2}$ versus V_{GB} when V_{GB} increases is due to the incomplete Debye screening, similarly for $I_P^{1/2}$ versus V_{GB} when V_{GB} decreases.

(3) In contrast, the 60mV per decade exponential roll-off of the electron and hole currents towards their very low values at flatbands, V_{GS} = 0V (electrons) and $V_{GS} = V_{DS}$ (holes) in the BC-U_N and BC-U_P families respectively, is the indicator of over-the-barrier-injection and carrier-diffusion limited, like the n^+/i and p^+/i barriers, or the n^+/p and p/n^+ barrier of the n-inversion channel on p-base pMOST and the $n^+/p/n^+$ BJT, with barrier height controlled respectively by transverse MOS capacitor and by applied electrical potential to the n^+/p emitter and p/n^+ collector diodes. They are simulated in these numerical computations by applying the boundary condition to the electrochemical potential for electrons, BC-U_N, and for holes, BC-U_P. This simulation, used by all device theorists, has not been recognized as empirical or ideal contact models, by them or anyone and also not recognized previously by us.

(4) The electron volume channel current, $I_N \sim 10^{-20} \times V_{DS}$ saturates at $V_{GS} = -1$V for the BC-U_0 family. The proportionality to V_{DS} is the indicator that current is drift. The very low current indicates the diminishing channel conductance or channel electrical thickness and carrier concentration.

(5) The extremely low saturation current, 10^{-20} A/sq, is the indication of pinch-off of the electrical thickness of the volume channel with physical thickness, x_B, and the reduction of N from n_i at Flat-band to nearly zero at the pinch-off (actually cut-off, see next point). This is entirely consistent with the volume channel pinch-off mechanism of the impure-base junction-gate FET illustrated by Shockley in 1952[4].

(6) However, the flatband electron and hole currents, $I_{N\text{-FB}}$ and $I_{P\text{-FB}}$, can be easily computed by the back-of-the-envelope formula $I_{N\text{-FB}}(\text{A/sq}) = \mu_n \times qn_i \times x_B \times V_{DS} = 1.92 \times 10^{-12}$ A/sq $= I_{P\text{-FB}}$ (with $\mu_n \sim \mu_p \sim 400\text{cm}^2/(\text{V}\cdot\text{s})$ and $n_i \sim 10^{10}\text{cm}^{-3}$). If there is carrier screening of the controlling electric field from the DC voltage applied to the two gates, then the saturation current given by (5) should be close to the flatband value. However, the back of the envelope flatband current for the electron or hole channel is $\sim 1.92 \times 10^{-12}/2 \times 10^{-20} = 10^8$ larger than the computer computed pinch-off or cut-off current. This is accounted for from the vanishing screening of the gate charge or gate electric field by the few mobile electrons and holes or carriers in the pure-base. This is estimated by the ratio of the oxide capacitance and the Debye capacitance, $(C_O/C_D)^2 = (\varepsilon_0/\varepsilon)^2(L_D/x_O)^2 = (3.9/11.7)^2 \times (26\mu\text{m}/1.5\text{nm})^2 = 3.4 \times 10^7$ which confirms the observed ratio in the range of 10^8. Thus, for the pure silicon base, the volume channel current corresponds to the cut-off of the pure volume channel, rather than to the pinch-off of the impure volume-channel of impure-base-body of the junction-gate FET.

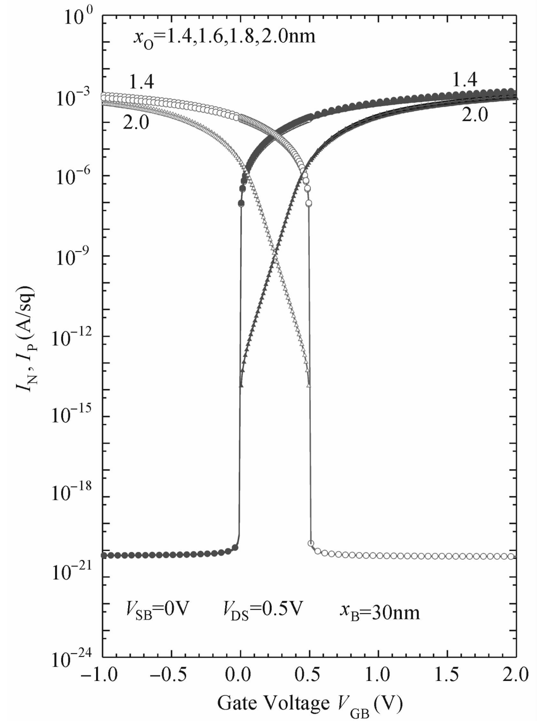

Fig. 2　Transfer DC characteristics of a BiFET of two MOS gates and a pure base, with x_O varied. The curves with triangle symbols have the electrochemical potential boundary conditions, while the curves with circle symbols have the electric potential boundary conditions.

(7) The hole volume channel current, I_P saturates to 0.09×10^{-20} A/sq at $V_{GS} = +2$V and $V_{DS} = +0.1$V which rises to 1.2×10^{-20} A/sq at $V_{DS} = +1.0$V. These two values are not identical to those of I_N. This difference is a reflection of the unequal final recursive iteration number of I_N and I_P using the zig-zag recursive iteration algorithm.

3.3　Gate-Oxide and Base Thickness Dependences

The I_N and I_P versus V_{GS} shown Fig. 1 with V_{DS} as the parameter, is now given in Fig. 2 with gate oxide thickness as a parameter, and in Fig. 3 with base thickness as a parameter. There is only slight oxide thickness dependence shown in Fig. 2, while Fig. 3 shows that the pinch-off or cut-off drift current is proportionally to the base thickness, x_B, as expected from the simple resistance model with a drift current.

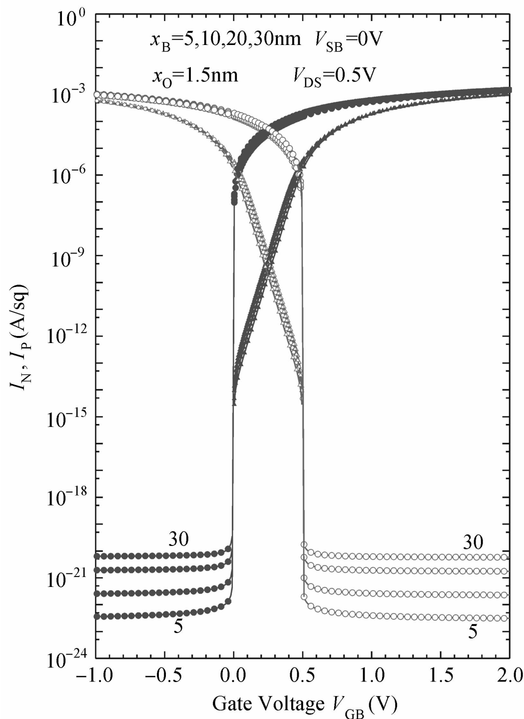

Fig. 3 Transfer DC characteristics of a BiFET of two MOS gates and pure base, with x_B varied. The curves with triangle symbols have the electrochemical potential boundary conditions, while the curves with circle symbols have the electric potential boundary conditions.

4 Summary

The bipolar solutions of the bipolar MOS field effect transistor with tied-identical-double gate on thin silicon pure-base are obtained in the linear range with the simultaneous presence of both electron and hole channels. The numerical results of 20-decades of electron and hole currents (10^{-22} to 10^{-2} A/Square) over the applied gate voltage range of $V_{GS} = -1V$ to $+2V$, cover the subthreshold and above-threshold surface channel ranges and also pinch-off volume channel range of both the electron and hole currents. Details including the current saturation range, $V_{DS} \geqslant V_{GS} \geqslant 0$, which requires the division of the channel length into two sections, described by equations (67) to (70), will be described in a future report in this series.

Acknowledgment We thank Professors Xing Zhou (Nanyang Technological University, Singapore) Chenming Hu (University of California, Berkeley), Gennady Gildenblat (Arizona State University) and Mitiko Miura-Mattausch (Hiroshima University) and Dr. Colin McAndrew (Freescale Semiconductor Corporation), and Drs. Jin Cai, Tak H. Ning, Lewis M. Terman, and Hwa-Nien Yu (all of IBM Thomas J. Watson Research Center) for encouragements, comments and suggestions. We further thank Professors Marcel D. Profirescu (University Politechnica of Bucharest, Romania), Adelmo Ortiz-Conde and Francisco J. Garcia Sanchez (Universidad Simon Bolivar, Venezuela), Juin J. Liou (University of Central Florida, USA), and Huang Ru (Peking University) for inviting us to present our results at their IEEE-EDS-sponsored mini-colloquium and IEEE-co-sponsored international conferences, NADE, MINI@Cancun, ICCDCS and ICSICT. We also thank Professor and Academician Wang Yang-yuan (Peking University) for his supports which have enabled us to undertake this study.

References

[1] Chih-Tang Sah and Bin B. Jie, "Bipolar Theory of MOS Field-Effect Transistors and Experiments," Chinese Journal of Semiconductors, 28(10), 1497 - 1502, October 2007. (CJS00)

[2] Chih-Tang Sah and Bin B. Jie, "The Bipolar Field-Effect Transistor Theory: I. Electrochemical Current Theory (Two-MOS-Gates on Pure-Base)," Chinese Journal of Semiconductors, 28(11), 1661 - 1673, November 2007. (CJS01)

[3] Bin B. Jie and Chih-Tang Sah, "The Bipolar Field-Effect Transistor Theory: III. Short- Channel Electrochemical Current Theory (Two-MOS-Gates on Pure-Base)," Journal of Semiconductors, 29(1), 1 - 11, January 2008. (CJS03)

[4] William Shockley, "A Unipolar 'Field Effect' Transistor," Proceedings of the IRE, 40(11), 1365 - 1376, November 1952.

[5] Chenming Hu, "From CMOS to Nanotechnology," Keynote, 17th Annual IEEE/SEMI Advanced Semiconductor Manufacturing Conference, May 22 - 24 2006, Boston, Massachusetts.

[6] Chih-Tang Sah and Bin B. Jie, "The Bipolar Theory of the Field-Effect Transistors: X. The Fundamental Physics and Theory (All Device Structures)," Journal of Semiconductors, 29(4), 613 - 619, April 2008. (CJS10) Preceding paper.

[7] Chih-Tang Sah and Bin B. Jie, "The Theory of Field-Effect Transistors: XI. The Bipolar Electrochemical Currents (1-2-MOS-Gates on Thin-Thick Pure-Impure Base," Journal of Semiconductors, 29(3), 397 - 409, March 2008. (CJS11)

[8] William Shockley, "The Theory of p-n junctions in Semiconductors and p-n Junction Transistors," Bell System Technical Journal 28(7), 435 - 489, July 1949.

双极场引晶体管：V. 双极电化电流理论（双 MOS 栅纯基）*,**

揭斌斌[1,†] 薩支唐[1,2,3,†]

（1 北京大学，北京 100871）

（2 佛罗里达大学，佛罗里达州，Gainesville FL32605，美国）

（3 中国科学院外籍院士，北京 100864）

摘要： 本文报告用双极场引晶体管(BiFET)电化电流解析理论计算的内禀结构直流特性，晶体管有两块等同 MOS 栅，纳米厚度纯硅基，没有产生复合和俘获.用交叉双路或 Z 形单路递归循环算法，很快得到三个势变量的数字解：静电势，电子和空穴电化学势，从而算出电子和空穴表面和体积沟道电流.三种势边界条件主导地影响内禀结构直流特性，用 20 个量级跨度电流说明.(10^{-22}～10^{-2} A/□，迁移率 400cm^2/(V・s)，1.5nm 厚栅氧化层，30nm 厚纯基)强表面沟道内载流子空间电荷限制飘移电流起主导作用，除此以外理论上还观察到，体积沟道物理夹断导致经典飘移电流饱和，因德拜长度(25μm)远大于器件尺寸(25nm)，纯基内少量电子和空穴载流子屏蔽消失导致纯基内体积沟道完全切断.这种切断是从在 1952 Shockley 结栅场引晶体管理论中描述的非纯基体积沟道物理夹断推理而来.

关键词： 双极场引晶体管理论；递归循环；电子和空穴电化学势；静电势；边界条件

PACC： 7340Q **EEACC：** 2560S；2560B

中图分类号： TN386.1 **文献标识码：** A **文章编号：** 0253-4177(2008)04-0620-08

---

* 该研究及揭斌斌由 CTSAH Associates (CTSA) 资助.CTSA 由薩故夫人张淑南创建.记念她七十周年.

** 薩支唐写成此摘要基于揭斌斌的现代语初稿.感谢潘胜和北京大学原物理系教师赵立群和潘桂明的修改建议.

† 通信作者.Email：bb_jie@msn.com and tom_sah@msn.com

2008-03-25 收到，2008-03-28 定稿

©2008 中国电子学会